Nanoscience and Nanotechnology Letters
Vol. 10, 1–6, 2018

Application of Laser-Induced Plasma Spectroscopy to Diffusion of Cu/Sn–Pb Metal Composites

Ji-Hun Kim, Sangwoo Yoon, Woo-Tae Park, and Joohan Kim*

Department of Mechanical Engineering, Seoul National University of Science and Technology, Seoul, 01811, Korea

In this study, we analyzed the diffusion characteristics of metal composites using laser-induced breakdown spectroscopy (LIBS). We confirmed and quantified the diffusion at the interface between the two metals, which we prepared by soldering followed by heat treatment. The advantage of measuring the spatial distribution of the elements in the specimen using LIBS is that the laser material removal allows us to measure the elements at the interface. We compared the distributions obtained using the LIBS technique to those acquired using other elemental analysis methods, such as energy dispersive spectroscopy (EDS), and analyzed the characteristics of the elemental distributions. We analyzed the metal distributions obtained using the LIBS technique up to nanoscale and compared them to those obtained using the EDS method. In addition, we found defects at the interface, which we also analyzed using LIBS. We investigated the relationship between bonding and diffusion by evaluating the morphologies of fractures in the two metal diffusion layers.

Keywords: Laser-Induced Breakdown Spectroscopy, Diffusion, Micro-Nano Structures.

1. INTRODUCTION

Dissimilar metal combinations, or metal composites, are made by bonding different metals with the aim of improving the material's mechanical, electrical, or chemical properties. These metal composites are typically produced by creating a heterojunction between two different materials with energy or bonding agents.[1] Dissimilar metal combinations form different compounds between the reinforcement metal and the substrate depending on the production conditions, and these compound layers grow into the interfacial layer by diffusion.[2] The material properties change as the interfacial layer grows, and chemical changes in the interface layer are liable to cause defects.[3,4] Therefore, it is necessary to study the reliability of the joints when fabricating combinations of dissimilar metals by heterobonding.[5–7] Studies on the reliability of bonding surfaces include evaluations of the characteristics of the element diffusion resulting from the chemical bonds between the elements in the bonded interface layers of dissimilar metal combinations. Energy dispersive spectrometry (EDS) or X-ray diffraction (XRD) can be used to measure the diffusion of the elements in these materials.[8,9] It is necessary to preprocess the specimens prior to EDS. For the elemental measurement inside the material, it is necessary to process the surface with the correct depth through the surface corrosion process. However, it is difficult and inaccurate to control. Furthermore, because the local portion of the surface of the material is measured by an electron beam, the measurements deviate significantly from the inspection position. Therefore, the error of the measured value is so large that it must be measured several times in order to obtain the average value. Elemental analysis methods that use X-rays, such as XRD, are accurate, but it is difficult to localize the X-rays and the measurement specimens are limited in size. The measurement inside the material using XRD has a disadvantage that the skin depth for measuring diffracted X-rays is limited. Recently, the development of laser source and optical spectroscopy techniques has in turn led to the development of methods for measuring the characteristics of materials using lasers. One of these techniques, component analysis through laser-induced breakdown spectroscopy (LIBS) has been studied extensively.[10,11] In LIBS, the specimen is ablated using a high-density focusing laser beam, and a plasma is produced. The elemental distribution of the material can be determined by analyzing the plasma spectroscopically. The high-density energy laser method enables us to measure the material as it is, because there is no need for a preprocessing step. In addition, precise removal of the target material is possible during induction of the plasma. This makes it possible to measure micro-holes in the surface of the original specimen in addition to its cross section, thereby allowing us to determine the elements inside the

*Author to whom correspondence should be addressed.

material.[12] It is also relatively easy to acquire the average value of the local signal by adjusting the size of the laser spot, since the range of the ablation material can be adjusted precisely.[13] Signal distortion may occur when measuring the diffusion element distribution using LIBS because of the material removal from the volume units by laser ablation. The behavior of the plasma generated by laser ablation also depends on the micro-nano structure of the material.[14] When plasma distortion occurs, the measured signal distribution may differ from that of the actual element.

In this study, we used LIBS to analyze the diffusion characteristics at the junction interface of a heterojunction between two metals. We used Cu and Sn–Pb alloys which can be bonded at low temperatures. We easily identified the diffusion phenomenon and observed elemental changes of Cu element diffusion into the alloy up to nanoscale. We evaluated the bonding characteristics of the bonding interface by investigating the mechanical properties of the bonding material by metal diffusion. We assessed the advantages and disadvantages of the LIBS measurement method by comparing the diffusion coefficients measured using LIBS and EDS.

2. EXPERIMENTAL DETAILS

We required a model of the diffusion so that we could confirm the diffusion behavior at the interfaces of heterogeneous junctions. If two uniform infinite bars with different compositions are in contact, their materials diffuse. The spatial distribution of the elemental concentration over time can be obtained using Fick's law, as follows

$$C(x,t) = C_o \int_{-\infty}^{0} \frac{e^{-((x-\hat{x})^2/4Dt)}}{\sqrt{4\pi Dt}}\, d\hat{x}$$

where, x is the position, $\hat{x}$ is the position in the initial source location, D is the diffusion coefficient, t is time, and C_o is the initial concentration of the element. We initially define the concentration at $x > 0$ to be zero. Therefore, $C(x,0)$ is zero. To obtain the solution of the governing equations above, the parameter u can be defined as

$$u = \frac{x-\hat{x}}{2\sqrt{Dt}}$$

The first equation can be rewritten as a function of u as follows

$$C(x,t) = \frac{C_o}{2}\left(\frac{2}{\sqrt{\pi}}\int_0^{\infty} e^{-u^2}\, du - \frac{2}{\sqrt{\pi}}\int_0^{x/2\sqrt{Dt}} e^{-u^2}\, du\right)$$

This equation is combined with the basic form of the error function and the diffusion equation is written as

$$C(x,t) = \frac{C_o}{2}\mathrm{erf}c\left(\frac{x}{2\sqrt{Dt}}\right)$$

According to the diffusion equation obtained, the diffusion coefficient can be calculated by approximating the experimental data obtained from the diffusion element analysis.[15] In particular, when a compound is formed as the result of diffusion, the assumption that one element diffuses into another element becomes incorrect, and the diffusion concentration is no longer calculated using the above equation. However, at this time, if the compound is sufficiently thick, it can be approximated by a Gaussian distribution.[16]

Cu and Sn–Pb alloys were used in the heterojunction experiments. Two metal plates were bonded to each other and a furnace soldering process was used to induce diffusion. The Sn–Pb alloy component consisted of 60 wt% Sn and 40 wt% Pb, and the phase diagram confirmed the eutectic temperature of 183 °C and the dissolution temperature of 190 °C.[17] The temperature of the furnace soldering was selected to be 185 °C. At 185 °C, Pb atoms are solid and Sn atoms are liquid. When diffusion occurs in this state, the compound thickness becomes irregular due to the mass convection. The specimens were heat-treated at this temperature for 10, 30, and 60 hours. The diffusion coefficient between Cu and Sn at 185 °C is reported to be 2.56×10^{-16} m^2/s.[18] To measure the diffusion coefficient using LIBS, we fabricated a sandwich structure from Cu/Sn–Pb/Cu which gave a heterogeneous metal bonding material. The diffusion type of the interface was first confirmed using an optical microscope and a scanning electron microscope (SEM). Tensile tests were also carried out to confirm the mechanical properties of the bond interface as a function of diffusion. The experimental setup of the laser-induced plasma spectrometer used for measuring the distribution of the elements is shown in Figure 1. A neodymium-doped yttrium aluminum garnet (Nd:YAG) pulsed laser with a wavelength of 266 nm was used. The laser energy per pulse was 25 mJ and the pulse width was 5 ns. We ablated the surface of the material by irradiating the laser onto it through a focusing lens and collecting and analyzing the generated plasma signal of the material. When the energies of the electrons stabilized by transitioning from the excited state into the ground state, the wavelength and size of the corresponding spectral lines varied

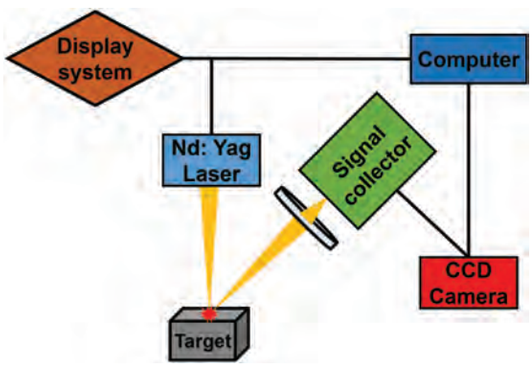

Fig. 1. Schematic of LIBS.

depending on the element. We determined the specific elements in the diffusion layer by comparing the wavelengths and sizes of the emitted light to the intrinsic energy levels of the constituent atoms. LIBS is capable of both laser beam ablation in the direction of the interior of the material and cross-sectional scanning, and of one-shot generation of micro-sized holes with a depth of a few hundred nanometers. In this way, we can determine the distribution of the elements as a function of the depth of the material in three dimensions. We evaluated the advantages and limitations of LIBS by comparing the results of the LIBS experiments to those of the EDS elemental analysis.

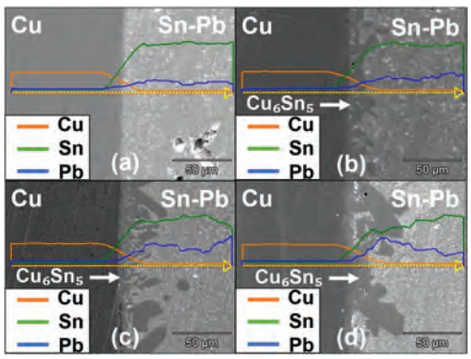

Fig. 3. EDS images of (a) baseline, (b) 10 hours, (c) 30 hours, and (d) 60 hours heat treated specimen.

3. RESULTS AND DISCUSSION

Figure 2(a) shows the thickness of the compound layer of the diffused specimen with respect to the heat treatment time. The degree of diffusion increased as the heat treatment time increased. We also measured the tensile yield stress to confirm the mechanical properties of the bonded specimen, as shown in Figure 2(b). According to our analysis of the thickness of the diffusion layer and the magnitude of the yield stress, which we measured by annealing, the yield stress decreased with increasing diffusion time. Defects occur on the Sn–Pb alloy at a distance from the diffusion interface. This phenomenon can be explained by the Kirkendall effect. As Cu is the predominant diffuser in the production of Cu/Sn–Pb compounds, Cu compounds are mainly produced by diffusion. At this time, the element that is not part of the compound evolves into a supersaturated state, and this increases the rate of defect formation outside the diffusion layer.[19] We used heat treatment to confirm the increase in size of the defects in the heterogeneous specimens. These defects appeared because many Kirkendall voids grew and coalesced into large dislocations. This also caused the density near the interface to change. We observed crack growth along the grain boundaries of the non-diffusing body in both Cu and the Sn–Pb alloy. However, once the compound had formed, the boundaries of the crack propagation became unclear and we observed cracks between the Cu and the compound. Taken together, it can be concluded that the Kirkendall void effect, which is caused by the differences between the diffusion coefficients of the elements, caused the initial cracks and lead the specimens to deteriorate.

For the comparative analysis of the diffusion measurements obtained using LIBS, we performed diffusion layer analysis using an existing element detection method, namely EDS. We verified that the distribution of the elements changed by taking elemental measurements of the diffuser and the base metal. The microstructures and element distributions of the boundary layer obtained using EDS are shown in Figure 3. The distributions of the elements can be deduced by observing the formation of compounds such as Cu_6Sn_5 at the Cu/Sn–Pb junction interface. When these compounds formed, the Pb element was detected later than the Sn, and then, the signal increased. This is presumed to be due to the local increase in the elemental distribution of the base material region caused by the formation of the compound. We also observed that each element was linearly distributed by the detection limit even when no diffusion occurred. According to the EDS measurements, the diffusion coefficients of the specimens after heat treatments with different durations were 1.31×10^{-15} m^2/s, 3.61×10^{-16} m^2/s and 1.74×10^{-16} m^2/s after 10, 30 and 60 hours respectively. These are not the average of the data and they are just obtained through a single inspection. So it does not represent the diffusion effect

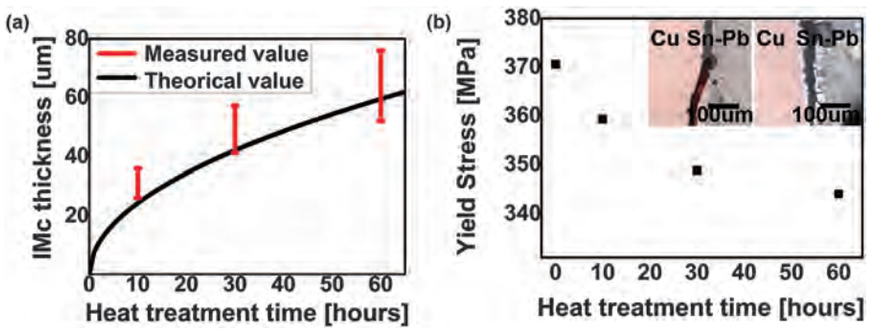

Fig. 2. Effect of heat treatment time on (a) thickness of intermetallic compound and (b) tensile yield stress.

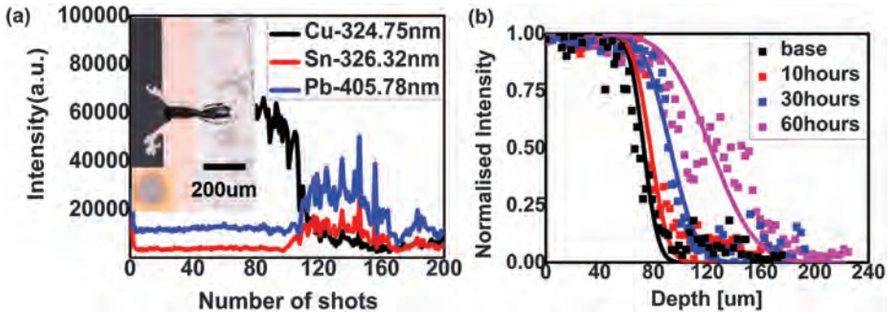

Fig. 4. Plasma intensity of (a) elements by laser shot and (b) Cu spectral lines at no, 10 h, 30 h, and 60 h heat treatment.

over time. The compound grows as the diffusion time during the heat treatment increases, but so do the deviations in the measured thickness of the compound. In addition, the error margin is too broad for it to be possible to quantify the overall diffusion using EDS.

The diameter of the micro pit was measured to be about 35 μm. In the depth measurements taken using LIBS, the initial plasma signal is somewhat distorted by the oxidized surface and surface roughness. Then, the plasma generation point becomes deeper as the micro pit becomes deeper, and the intensity of the plasma detected by the spectroscope decreases gradually. This phenomenon can be inferred from the transition in the measurement signal, as shown in Figure 4(a). For our analysis, we collected valid data and used these to correct the values of the plasma intensity at the diffusion interface. Figure 4(b) shows the spectral line peak of the Cu element of the specimen measured using LIBS with respect to the diffusion time. In the case of no diffusion, the Cu signal was constant, but the signal decreased as the Cu metal diffused. The strength of the Cu spectral line peaks of the specimens heat-treated at 185 °C for 10, 30 and 60 hours increased with the treatment time. In contrast to the results from the EDS analysis, the elemental LIBS measurements indicated the average elemental distribution even though the compound layer was not uniform. We confirmed which section of the specimens that diffused for 60 hours contained the Cu peak. This was presumed to be a Cu_6Sn_5 compound, and the decreasing signal gradient indicates that $D^{Cu-Cu_6Sn_5}$ and $D^{Cu_6-Sn_5-Sn}$ diffusion occurred.[20]

As in the case of the EDS measurements, the LIBS measurements indicated that the elements were linearly distributed, even when diffusion did not occur at the metal composite interface. The reason for this was that the distribution of the intensity of the laser energy irradiated on the material is Gaussian; this determined the ablation characteristics of each material. Therefore, when inspecting the interior of the material, the plasma signal generated at the Cu/Sn–Pb junction was distorted by the characteristics of the beam profile. Sn–Pb alloys are softer than Cu, so laser ablation is easier in this case. Therefore, when the Gaussian laser beam reached the interface layer, alloy ablation was easier than Cu ablation, and this may have caused errors in the values measured through the plasma. We improved the accuracy of the obtained element distribution by correcting these distorted signals up to nanoscale. The improved distribution is shown in Figure 5.

We approximated the data curve obtained using LIBS measurements as an error function. We then calculated the diffusion coefficient numerically using the following equation, based on the assumption that the intensity of the spectrum was proportional to the concentration of the element,

$$\frac{C}{C_o} = \mathrm{erf}\,c\left(\frac{x}{2\sqrt{Dt}}\right)$$

The error function represents an infinite source. Since the initial compound generation does not affect the infinite

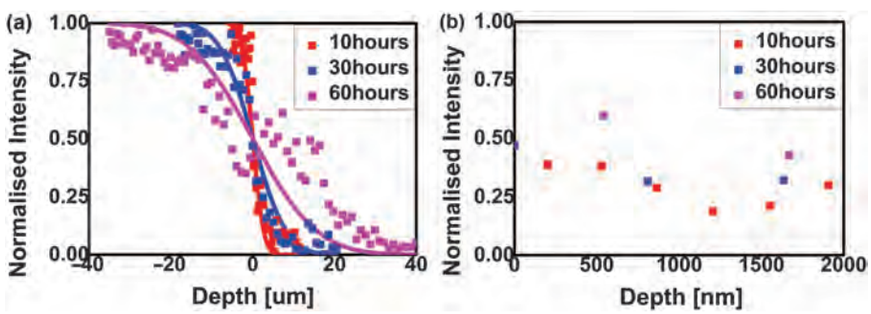

Fig. 5. (a) Calibrated profile of Cu spectral lines at 10 hours, 30 hours, and 60 hours heat treatment time and (b) calibrated profile of Cu spectral lines with nanoscale.

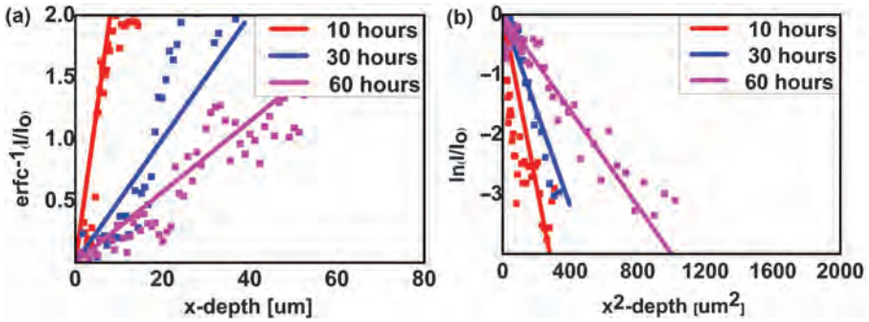

Fig. 6. Calibrated data curve fitting of (a) inverse error function and (b) inverse Gaussian function.

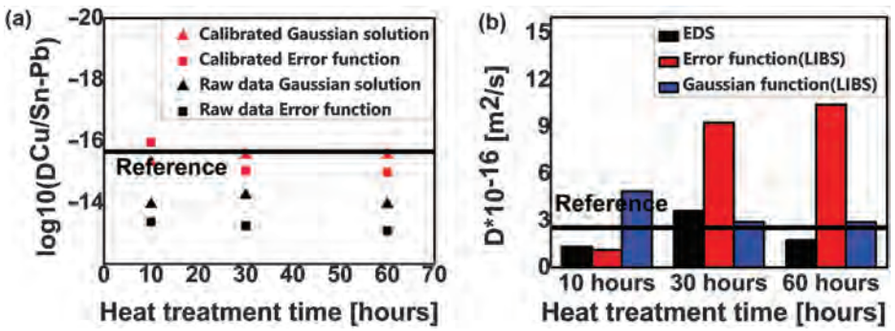

Fig. 7. (a) Diffusion coefficient with respect to the heat treatment time and (b) comparison of EDS and LIBS.

source, the initial diffusion can be approximated as an error function.[21] However, the source can no longer be assumed to be infinite once the generation of the Cu/Sn compound has been initiated, and the distribution of the elements deviates from the distribution of the error function. In this case, the analysis can be performed by assuming that the element distribution is a Gaussian defined by the following equation,

$$\frac{C}{C_o} = \exp\left(-\frac{x^2}{4Dt}\right)$$

To compensate for distortion in the plasma signal, the measured data were corrected using a Cu/Sn–Pb junction that had not diffused. First, the raw and corrected data were fitted to an inverse error function, giving a gradient of $1/(2\sqrt{Dt})$, as shown in Figure 6. It also shows the curve fitted to the inverse Gaussian function, which had a gradient of $-1/(4Dt)$.

These gradients were used to calculate the diffusion coefficients. The diffusion coefficients calculated from both the raw and calibrated data are summarized in terms of the heat treatment time. Without correction, the effect of overlapping with the original signal was measured to be wider than the actual elemental distribution obtained from the plasma spectral line measurements. This caused large deviations and errors. However, it was possible to remove the background plasma signal distribution by correcting the signal distortions. This enabled us to obtain the correct diffusion coefficient (Fig. 7(a)). The diffusion coefficient obtained using the inverse error function was calculated to be 1.11×10^{-16} m^2/s because the compound thickness due to diffusion was assumed to originate from an infinite source. This value was more accurate than the 4.86×10^{-16} m^2/s obtained using the Gaussian solution. On the other hand, the source could no longer be assumed to be infinite as the thickness of the compound increased. In this case, the diffusion coefficient calculated using the error function was 1.04×10^{-15} m^2/s. The error associated with this value is large. However, when the Gaussian solution was applied, the diffusion coefficient converged to 2.86×10^{-16} m^2/s as the heat treatment time increased (Fig. 7(b)). As a result, LIBS could measure elemental distributions in the material with improved resolution. Compared to the EDS method, preprocessing was not required. In addition, LIBS was able to obtain an average value with a single measurement, which is similar to reference value. The minimum error was about 12% and this allowed us to quantify irregular diffusion phenomenon.

4. CONCLUSION

In this study, we used LIBS to quantify the diffusion phenomenon by measuring the formation of compounds by diffusion in the heterojunction of a Cu and Sn–Pb alloy. In addition, we investigated the effect of diffusion on the bonding layer by measuring the tensile yield stress of the compound layer. We also confirmed the role of diffusion at

the interface on crack initiation and growth tendency. The heterogeneous boundary layer was confirmed by SEM and we performed EDS analysis so that we could compare the results to those of the LIBS measurements. The diffusion coefficient was derived from the LIBS measurements by quantifying the size of the Cu plasma peak signal up to nanoscale. We corrected the distortion of the plasma signal in the LIBS analysis of the interfacial layer elements. This made it possible to obtain a reasonable value for the diffusion coefficient. When the thickness of the compound was small, it was appropriate to analyze the data by fitting them to the error function. However, the Gaussian fitting was more accurate when the thickness of the compound layer increased.

Acknowledgments: This research was supported by Basic Science Research Program through the National Research Foundation of Korea (NRF) funded by the Ministry of Education (2018R1D1A1B0741576).

References and Notes

1. Y. Kobayashi, Y. Yasuda, and T. Morita, *J. Sci. Adv. Mater.* 1, 413 (**2016**).
2. Q. Lai, L. Zhang, C. Chen, and J. K. Shang, *J. Mater. Sci. Technol.* 28, 379 (**2012**).
3. J. Wang, Q. Wang, Z. Liu, Z. Wu, J. Cai, and D. Wang, *Appl. Surf. Sci.* 384, 200 (**2016**).
4. M. L. Huang, N. Kang, Q. Zhou, and Y. Z. Huang, *J. Mater. Sci. Technol.* 28, 844 (**2012**).
5. F. Dugal and M. Ciappa, *Microelectron. Reliab.* 76, 460 (**2017**).
6. M. L. Huang, A. J. Zhang, H. T. Ma, and L. D. Chen, *J. Mater. Sci. Technol.* 30, 1235 (**2014**).
7. J. H. Dai, B. Jiang, C. Peng, and F. S. Pan, *J. Alloy. Compd.* 710, 260 (**2017**).
8. T. Hu, H. Chen, and M. Li, *Mater. Design* 108, 383 (**2016**).
9. J. Wang, Y. Li, P. Liu, and H. Geng, *J. Mater. Process Tech.* 205, 146 (**2008**).
10. T. O. Nagy, U. Pacher, A. Giesriegl, M. J. J. Weimerskirch, and W. Kautek, *Appl. Surf. Sci.* 418, 508 (**2017**).
11. Y. Dixit, M. P. Casado-Gavalda, R. Cama-Moncunill, X. Cama-Moncunill, M. Markiewicz-Keszycka, F. Jacoby, and C. Sullivan, *J. Food. Eng.* 216, 120 (**2018**).
12. M. Suchoňová, J. Krištof, M. Pribula, M. Veis, F. L. Tabarés, and P. Veis, *Fusion Eng. Des.* 117, 175 (**2017**).
13. S. H. Choi, C. S. Kim, K. Y. Jhang, and W. S. Shin, *Trans. Kor. Soc. Mech. Eng. A* 35, 1105 (**2011**).
14. R. Gaudiuso, *Spectrochim. Acta B* 123, 105 (**2016**).
15. S. E. Hosseini, *J. Iron. Steel. Res. Int.* 19, 71 (**2012**).
16. C. Ararat-Ibarguen, R. A. Pérez, and M. Iribarren, *Measurement* 55, 571 (**2014**).
17. J. S. Lee, Y. S. Ahn, G. H. Kang, and J. P. Wang, *Appl. Surf. Sci.* 415, 137 (**2017**).
18. W. S. Hong, W. S. Kim, N. C. Park, and K. B. Kim, *J. Weld.* 25, 82 (**2007**).
19. K. N. Tu and R. D. Thompson, *Acta Metall. Mater.* 30, 947 (**1982**).
20. Y. Yuan, Y. Guan, D. Li, and N. Moelans, *J. Alloy. Compd.* 661, 282 (**2016**).
21. C. Ararat-Ibarguen, C. Corvalán , N. Di Lalla, M. Iribarren, R. Pérez, and E. Vicente, *Procedia. Mater. Sci.* 8, 1004 (**2015**).

Received: 9 May 2018. Accepted: 26 June 2018.